JOURNAL OF SOLID STATE CHEMISTRY 91, 312–322 (1991)

Synthesis and Structure of $Ln_2Ta_3Se_2O_8$ (Ln = La, Ce, Pr, Nd)

THEODORE D. BRENNAN, LORRAINE E. ALEANDRI, AND JAMES A. IBERS

Department of Chemistry, Northwestern University, Evanston, Illinois 60208-3113

Received August 21, 1990

A series of compounds $Ln_2Ta_3Se_2O_8$ (Ln = La, Ce, Pr, and Nd) has been prepared and characterized. $Pr_2Ta_3Se_2O_8$ is orthorhombic, space group D_{2h}^{12} – *Pnnm*, with unit cell constants a = 9.882(3), b = 11.774(3), c = 7.601(2) Å, T = 111 K, Z = 4. The structure has been solved and refined from single crystal X-ray diffraction data. The structure, including the oxygen content and positions, has been confirmed from neutron diffraction powder data. The asymmetric unit contains two independent Pr atoms, two independent Ta atoms, two independent Se atoms, and five independent O atoms. The Pr atoms are in tricapped-trigonal prismatic sites enclosed by seven O and two Se atoms. One Ta atom is in a distorted octahedral site surrounded by six O atoms, and the other Ta atom is also in a distorted octahedral environment but has two *trans* O and four Se atoms in its coordination sphere. The structure shows a three-dimensional arrangement and is built up from layers of the Pr tricapped-trigonal prisms alternating with layers of the Ta octahedra. The other members of the series, Ln = La, Ce, and Nd, have the same structure, as judged from the similarity of their X-ray powder patterns with that of $Pr_2Ta_3Se_2O_8$.

Introduction

Few quaternary lanthanide transition-metal oxysulfide or oxyselenide compounds are known. Compounds have been reported in the *Ln*/ *M*/ S,Se/ O systems, (*M* = Cu, Ag, Ga, In, Ge, Sn, As, Sb, and Bi), and are typically layered materials with (Ln_2O_2) and (M_xQ_y) slabs (*1*). A series of compounds with the stoichiometries $Ln_{2n-2}U_2O_{2n}S_{n+1}$, where n = 2–6, has recently been reported; the n = 2 and n = 3 members are related to the $Ce_4O_4S_3$ and $Ce_6O_6S_4$ structures, respectively (*2–4*). *M* = Cr, V compounds are known; their structures are three-dimensional. There are two types of structures known for *M* = Cr, orthorhombic $LaCrOS_2$ (*5*) and $LaCrOSe_2$ and monoclinic $LnCrOS_2$ (*Ln* = Ce . . . Sm) (*6*). $LaCrOS_2$ and $LaCrOSe_2$ are ferromagnetic (*7*), attributed to super–superexchange interactions, while $NdCrOS_2$ is antiferromagnetic and undergoes a spin-flop transition (*8*). The one known quaternary V compound, $La_5V_3O_7S_6$, contains both V^{+5} and V^{+3} sites (*9*). In the *M* = Cr, V structures the lanthanide atoms are found in tricapped-trigonal prismatic sites and the transition metals are in octahedral sites. Here we report the synthesis and structures of the new quaternary oxyselenide compounds $Ln_2Ta_3Se_2O_8$ (*Ln* = La, Ce, Pr, Nd).

Experimental

Synthesis. Praseodymium sesquiselenide, Pr_2Se_3, was prepared from the ele-

0022-4596/91 $3.00

mental powders Pr (REACTON, 99.9%) and Se (Aldrich, 99.999+%) in evacuated quartz tubes heated at 775 K, 1075 K, and then 1275 K. A combination of Pr_2Se_3, Ta (AESAR 99.98%), and Se powders in a 1:6:9 ratio was loaded into a quartz tube that was subsequently evacuated to 10^{-5} Torr, sealed, and heated at 1275 K in an attempt to make a new ternary chalcogenide. The oven thermocouple failed, causing the furnace to go above 1475 K. Black powder and rectangular black prisms were produced. Analysis of two such prisms with the microprobe of an EDAX-equipped Hitachi S-570 scanning electron microscope revealed the presence of Pr and Ta and a low amount of Se. A reaction mixture of Ce_2Se_3, Ta, and Se powders in a 1:6:9 ratio, which was in the furnace with the Pr_2Se_3/Ta/Se reaction, also produced small rectangular black prisms which EDAX analysis showed contained Ce, Ta, and Se. The lack of reliable standards prevented quantitative analysis. A single-crystal X-ray diffraction study was then carried out on a small prism from the Pr reaction. The structure deduced was of the new quaternary $Pr_2Ta_3Se_2O_8$, with oxygen presumed to have been extracted from the silica. A sample was then prepared in order to carry out a neutron diffraction powder study to confirm the X-ray structure and oxygen content. A powder sample of $Pr_2Ta_3Se_2O_8$ was prepared in a more rational way by the reaction of Pr_7O_{12}, Ta_2O_5, Ta, and Se powders in a 0.87:1.4:6.2:6 ratio at 1375 K.

$La_2Ta_3Se_2O_8$ and $Nd_2Ta_3Se_2O_8$ single crystals were prepared as black rectangular prisms by the reaction of La_2Se_3, Ta_2O_5, and Ta (1:1:1) at 1475 K for 7 days and Nd_2Se_3, Ta_2O_5, Ta, and Se (1:1:1:1) at 1475 K for 3 days. With the use of $Pr_2Ta_3Se_2O_8$ as a standard reference, EDAX elemental analysis indicated La/Ce/Nd, Ta, and Se ratios as expected for $Ln_2Ta_3Se_2O_8$. Variable temperature magnetic susceptibility measurements were made on a powder sample of $La_2Ta_3Se_2O_8$ that showed no trace of impurities as judged from X-ray diffraction powder patterns recorded with an Enraf–Nonius Model FR552 Guinier camera. This sample had been prepared by the reaction of La_2O_3, Ta_2O_5, Ta, and Se powders (1:1:1:3) at 1475 K for 4 days in an evacuated carbon-coated quartz tube. The powder was washed with 6 *M* HCl before susceptibility data were collected. $Ln_2Ta_3Se_2O_8$ crystals are best prepared by the reaction of equimolar amounts of Ln_2Se_3, Ta_2O_5, and Ta powders at 1475 K; $Ln_2Ta_3Se_2O_8$ powders are best prepared by the reaction of Ln_2O_3, Ta_2O_5, and Ta powders with a slight excess of Se powder at 1375–1475 K in a carbon-coated quartz tube.

X-ray diffraction analysis of $Pr_2Ta_3Se_2O_8$. The unit cell parameters for $Pr_2Ta_3Se_2O_8$ were determined from least-squares refinement of 15 reflections in the range $23° \leq 2\Theta$ (Mo$K\alpha_1$) $\leq 35°$ that had been automatically centered on a Picker FACS-1 diffractometer at 111 K. Additional data collection parameters and crystallographic details are given in Table I. During data collection six standard reflections measured after every 100 reflections showed no significant variation in intensity. An examination of intensity data revealed Laue symmetry *mmm* and systematic absences $0kl$, $k + l$ odd and $h0l$, $h + l$ odd, consistent with space groups *Pnn*2 and *Pnnm*. All calculations were performed on a Harris 1000 computer with methods and programs standard for this laboratory (*10*). Conventional atomic scattering factors (*11*) were used and anomalous-dispersion corrections (*12*) were applied. The processed data were corrected for absorption effects. The hkl and $hk\bar{l}$ reflections were averaged to give a merging R index of 6.1%. In view of the magnitude of the absorption correction we take this good agreement to support the choice of the centrosymmetric space group *Pnnm*. Subsequent refinement confirms this choice. The initial positions for the heavy

TABLE I

X-RAY DATA PARAMETERS FOR $Pr_2Ta_3Se_2O_8$

Formula	$Pr_2Ta_3Se_2O_8$
Molecular weight	1110
Space group	D_{2h}^{12}-*Pnnm*
a (Å)	9.882(2)
b (Å)	11.774(3)
c (Å)	7.601(2)
V (Å^3)	884
Z	4
T (K)	111[b]
Crystal volume (mm^3)	3.89×10^{-4}
Crystal shape	Prism ≈ 0.09 × 0.07 × 0.08 mm bound by (011), (01$\bar{1}$), (0$\bar{1}\bar{1}$), (01$\bar{1}$), (001), (01$\bar{2}$), ($\bar{1}$00), (100), (10$\bar{1}$), (10$\bar{1}$), (101), ($\bar{2}$10)
Radiation	Mo$K\alpha$ graphite monochromatized ($\lambda(K\alpha_1)$ = 0.7093 Å)
Linear absorption coefficient (cm^{-1})	554
Transmission factors	0.037–0.107[a]
Detector aperture (mm)	Horizontal, 5.5; vertical, 5.5, 32 cm from crystal
Scan type	2Θ
Scan speed	2°/min in 2Θ
2Θ limits (deg)	$3 \leq 2\Theta$ (Mo$K\alpha_1$) ≤ 64
Background counts	10 sec at each end of scan[c] with rescan option
Data collected	$+h, +k, \pm l$
p factor	0.04
No. of variables	38
No. of unique data	1772
No. of unique data with $F_0^2 > 3\sigma(F_0^2)$	1105
$R(F^2)$	0.079
$R_2(F^2)$	0.112
R (on *F*, $F_0^2 > 3\sigma(F_0^2)$)	0.040
Error in obs. of unit weight (e^2)	1.12

[a] The analytical method as employed in the Northwestern absorption program AGNOST was used for the absorption correction (*23*).

[b] The low-temperature system is based on a design by J. C. Huffman (*24*).

[c] The diffractometer was operated under the Vanderbilt disk-oriented system (*25*).

atoms Pr, Ta, and Se were determined by the direct methods program SHELX-86 (*13*). The oxygen atoms were located in subsequent difference electron density maps. The final cycle of isotropic refinement on F_0^2 resulted in values of R (F_0^2) of 0.080 and R_w (F_0^2) of 0.112. The final difference electron density map shows no features greater than 1.1% the height of a Ta atom. The program TIDY (*14*) was used to standardize the crystal structure according to the rules formulated by Parthé and Gelato (*15*). The final positional and thermal parameters are given in Table II. Structure amplitudes are given in Table III.[1]

Neutron Diffraction analysis of $Pr_2Ta_3Se_2O_8$. Neutron diffraction data on a 3.5-g sample of $Pr_2Ta_3Se_2O_8$ powder were collected at ambient temperature on the General Purpose Powder Diffractometer of the IPNS Facility at Argonne National Laboratory (*16*). Data were collected from the 2Θ = 148°, 90°, and 60° detector banks. Only 90°-scattering data were used in the refinement, as a compromise between resolution and low-angle reflections as these reflections are very sensitive to oxygen placement. Data reduction and least-squares refinement were carried out with the use of the programs of the IPNS Rietveld profile analysis package for time-of-flight data from a spallation pulsed neutron source (*17*). Details on data collection and refinement results are given in Table IV. The initial atomic positions for $Pr_2Ta_3Se_2O_8$ were taken from the single-crystal X-ray structure and the starting unit cell parameters from those obtained at room temperature from a Guinier X-ray powder pattern. Pr Ta_3O_9, a second phase in the neutron pow-

[1] See NAPS document No. 04836 for 15 pages of supplementary material. Order from ASIS/NAPS. Microfiche Publications, P.O. Box 3513, Grand Central Station, New York, N.Y. 10163. Remit in advance $4.00 for microfiche copy or for photocopy, $7.75. All orders must be prepaid. Institutions and Organizations may order by purchase order. However, there is a billing and handling charge for this service of $15. Foreign orders add $4.50 for postage and handling, $1.50 for postage of any microfiche orders.

TABLE II

X-RAY POSITIONAL PARAMETERS AND B (Å^2) FOR $Pr_2Ta_3Se_2O_8$

Atom	Wyckoff position	x	y	z	B (Å^2)
Pr(1)	4g	0.20868(10)	0.34251(9)	0	0.12(2)
Pr(2)	4g	0.72699(11)	0.14934(9)	0	0.13(2)
Ta(1)	8h	0.36452(5)	0.08388(4)	0.25018(7)	0.07(1)
Ta(2)	4e	0	0	0.28472(9)	0.12(1)
Se(1)	4g	0.02311(19)	0.13934(16)	0	0.20(3)
Se(2)	4g	0.51831(20)	0.33485(16)	0	0.24(3)
O(1)	8h	0.3026(9)	0.4748(8)	0.2352(11)	0.1(1)
O(2)	8h	0.0584(9)	0.3973(8)	0.2537(12)	0.1(1)
O(3)	8h	0.2857(10)	0.2249(8)	0.2518(13)	0.3(1)
O(4)	4g	0.3507(16)	0.0471(13)	0	0.5(2)
O(5)	4g	0.1336(15)	0.5513(12)	0	0.3(2)

der sample, was modeled as pseudotetragonal but without disordered oxygen atoms as in $LaTa_3O_9$ (*18*). The scale factors for the two phases and five background parameters were first refined. Then the positional parameters and overall B for $Pr_2Ta_3Se_2O_8$ were refined. Refinement of individual isotropic thermal parameters proved to be impossible, as some went slightly negative. The overall B for $PrTa_3O_9$ was also refined with the positional parameters fixed at those for $LaTa_3O_9$. At this point, the profile R (R_p) and weighted profile R (R_{wp}) values were 3.8% and 5.6%, respectively. The structure was then refined after in turn removing each of the oxygen atoms. This yielded R_p and R_{wp} values of 7.0% and 10.1% after removing atom O(1), 7.3% and 10.4% after atom O(2), 7.4% and 10.4% after atom O(3), 5.2% and 7.2% after atom O(4), and 5.3% and 7.3% after atom O(5). A smaller change occurred upon removing atoms O(4) or O(5) because they lie on mirror planes while the other oxygen atoms are at general positions and contribute more to the scattering. If both atoms O(4) and O(5) are removed from the model, the values obtained are R_p 7.6% and R_{wp} 10.5%. This displays the sensitivity of the data to oxygen scattering. Refinement of all O-atom occupancies while holding the heavy-atom occupancies fixed indicates that the O-atom sites are fully occupied to within 2%. In the

TABLE IV

NEUTRON DATA COLLECTION AND RIETVELD REFINEMENT

Formula	$Pr_2Ta_3Se_2O_8$	$Pr_{2/3}Ta_2O_6$
Molecular weight	1110	552
Space group	*Pnnm*	*P4/mmm*
a (Å)	9.8874(4)	3.8948(3)
b (Å)	11.8030(4)	—
c (Å)	7.6074(2)	7.8385(4)
V (Å^3)	887.80(4)	118.91(3)
Z	4	1
T (K)	298	298
Scan technique	Time-of-flight, GPPD of IPNS (ANL)	
Detector bank	(2θ = 90°)	
d-spacing limits	0.6993–4.0365	
No. of data points	3205	
No. of reflections	1499	146
No. of variables	32	4
Peak shape function	Jorgensen function	
Total No. variables	41	
$R(F^2)$	0.074	
R_p	0.038	
R_{wp}	0.056	
R_{exp}	0.025	
Scale factor	0.00047	0.00064
RF^2	0.074	0.117
Weight percentage	97.7%	2.3%

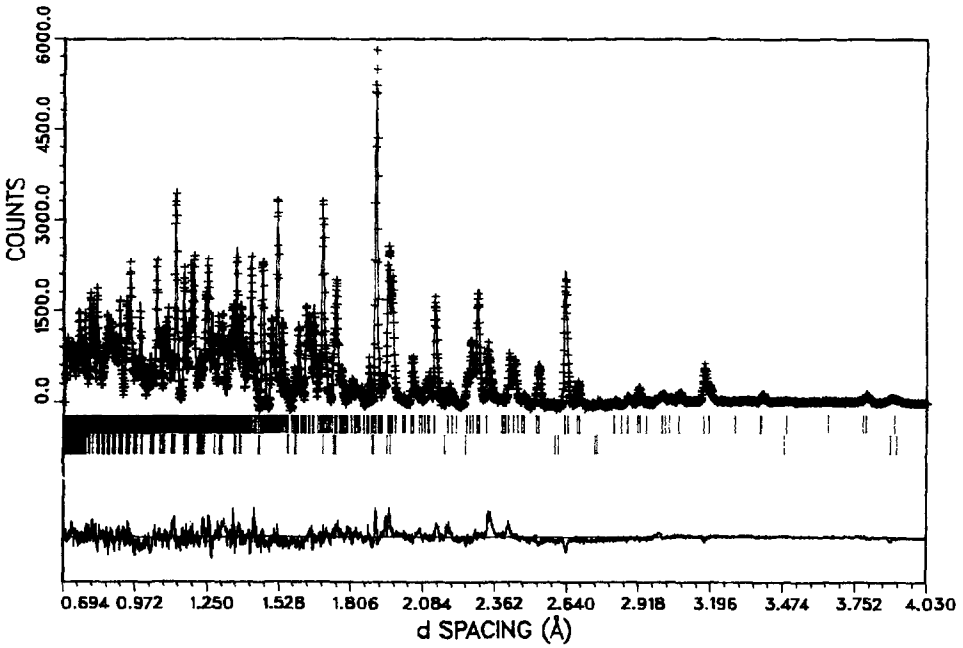

FIG. 1. Final Rietveld profile fit for $Pr_2Ta_3Se_2O_8$ with $PrTa_3O_9$ impurity: +, data points; solid line through data points, calculated profile; upper set of vertical lines below profile, the positions of all allowed reflections for $Pr_2Ta_3Se_2O_8$; lower set of vertical lines, allowed reflections for $PrTa_3O_9$. A difference plot appears at the bottom. The fitted background has been subtracted from both the observed and the calculated data.

final refinement the peak broadening parameters σ-1 and σ-2 for $Pr_2Ta_3Se_2O_8$ were also varied, and the refinement included all of the oxygen atoms. From the relative scale factors, $PrTa_3O_9$ is present in the sample at 2.3 wt% (*19*). Figure 1 shows the final Rietveld profile fit for refinement. The final positional parameters from the neutron data are given in Table V. Observed intensities are given in Table III.

X-ray Guinier powder photographs of $La_2Ta_3Se_2O_8$, $Ce_2Ta_3Se_2O_8$, and $Nd_2Ta_3Se_2O_8$ show the same pattern of intensities as found for $Pr_2Ta_3Se_2O_8$. Unit cell parameters for the new $Ln_2Ta_3Se_2O_8$ series of compounds are listed in Table VI.

In another series of experiments Pr_7O_{12}, Ta_2O_5, Ta, and Se powders in the appropriate ratios to get the stoichiometries of $Pr_2Ta_3Se_2O_6$, $Pr_2Ta_3Se_2O_7$, and $Pr_2Ta_3Se_2O_8$ were reacted at 1375 K. X-ray Guinier powder photographs of the reaction series showed the least amount of impurities present in the $Pr_2Ta_3Se_2O_6$ reaction products.

Physical measurements. Magnetic susceptibility measurements of $La_2Ta_3Se_2O_8$ were performed at 5 kG over the temperature range 5–250 K with a Quantum Design MPMS variable temperature SQUID magnetic susceptometer. Because we were interested in determining the electronic state of the Ta atoms, the La compound was chosen for magnetic measurements to avoid complications from *f* electrons. Gelatin capsules were used as sample holders. The sample weight was 43.5 mg. Data points were calculated by averaging four measurements at each temperature.

Two single crystals of $La_2Ta_3Se_2O_8$ mea-

TABLE V

NEUTRON POSITIONAL PARAMETERS FOR $Pr_2Ta_3Se_2O_8$[a]

Atom	Wyckoff position	x	y	z
Pr(1)	4g	0.2046(15)	0.3494(14)	0
Pr(2)	4g	0.7296(14)	0.1543(14)	0
Ta(1)	8h	0.3648(5)	0.0808(4)	0.2508(20)
Ta(2)	4e	0	0	0.2820(10)
Se(1)	4g	0.0230(11)	0.1355(7)	0
Se(2)	4g	0.5186(11)	0.3371(7)	0
O(1)	8h	0.3027(6)	0.4748(5)	0.2377(14)
O(2)	8h	0.0601(6)	0.3973(5)	0.2565(19)
O(3)	8h	0.2867(6)	0.2245(5)	0.2499(22)
O(4)	4g	0.3554(14)	0.0560(12)	0
O(5)	4g	0.1321(15)	0.5484(12)	0

[a] The refined value of the overall thermal parameter is $B = 0.23(4)$ Å^2.

suring in size 0.68 × 0.48 × 0.29 mm and 0.64 × 0.42 × 0.39 mm were mounted with Ag paint to Cu wires on a microscope slide. Two probe conductivity measurements along the c axis were then carried out with the use of a digital ohmmeter. Two-probe conductivities at 298 K were in the range of $1.4–2.7 \times 10^{-6}\ \Omega^{-1}\ cm^{-1}$. These conductivities are only approximate because of difficulty in measuring the dimensions of the crystal accurately. The contact resistances were taken to be negligible because of the low conductivity of the crystals.

Results

Oxygen content. The original reaction that produced crystals of $Pr_2Ta_3Se_2O_8$ contained no source of oxygen other than the quartz tube. The presence of oxygen, as revealed by the X-ray structure determination, was at first a surprise, but the resultant structure was very reasonable. However, earlier reactions with starting stoichiometries of $Pr_2Ta_3Se_2O_y$, $y = 6$, gave X-ray diffraction powder patterns with fewer lines from impurities than on patterns from $y = 7$ or 8. This suggested that $Pr_2Ta_3Se_2O_6$ might be the correct composition. The removal of one or more oxygen atoms had little effect on the X-ray structure refinement. Removal of atoms O(4) and O(5) increased $R(F_0)$ from 0.040 to 0.051. Neutron diffraction data, however, are more sensitive to oxygen content. The poor agreement for all other models in the Rietveld refinement of the neutron diffraction data confirms the $Pr_2Ta_3Se_2O_8$ model derived from the X-ray data.

TABLE VI

UNIT CELLS OF THE COMPOUNDS $Ln_2Ta_3Se_2O_8$[a]

$La_2Ta_3Se_2O_8$	9.929(4)	11.951(4)	7.666(3)	910
$Ce_2Ta_3Se_2O_8$	9.947(4)	11.848(1)	7.647(6)	901
$Pr_2Ta_3Se_2O_8$	9.910(2)	11.814(2)	7.624(2)	893
$Nd_2Ta_3Se_2O_8$	9.898(2)	11.777(3)	7.597(1)	886

[a] Guinier photography at $T = 298$ K.

Description of the structure. The structure of $Pr_2Ta_3Se_2O_8$ is described in terms of bond distances and angles in Table VII (X-ray results). A labeled view of the unit cell is provided in Fig. 2, and a stereoview of the unit cell is provided in Fig. 3. The structure comprises layers of octahedrally coordinated Ta atoms separated in the b direction by lanthanide cations occupying

TABLE VII

DISTANCES (Å) AND ANGLES (deg) IN $Pr_2Ta_3Se_2O_8$ FROM SINGLE-CRYSTAL X-RAY DATA

Pr(1)–O(3)	2×	2.482(10)	Pr(2)–O(4)		2.437(16)
Pr(1)–O(2)	2×	2.517(9)	Pr(2)–O(3)	2×	2.467(10)
Pr(1)–O(1)	2×	2.546(9)	Pr(2)–O(2)	2×	2.565(9)
Pr(1)–O(5)		2.568(14)	Pr(2)–O(1)	2×	2.597(9)
Pr(1)–Se(1)		3.014(2)	Pr(2)–Se(1)		2.929(2)
Pr(1)–Se(2)		3.061(2)	Pr(2)–Se(2)		3.004(2)
Pr(1)···Ta(1)		3.494(1)	Pr(2)···Ta(1)		3.460(1)
Ta(1)–O(3)		1.834(10)	Ta(2)–O(1)	2×	1.979(9)
Ta(1)–O(2)		1.929(9)	Ta(2)–Se(2)	2×	2.548(2)
Ta(1)–O(5)		1.937(3)	Ta(2)–Se(1)	2×	2.725(2)
Ta(1)–O(4)		1.955(4)	Ta(1)···Ta(1)		3.327(1)
Ta(1)–O(1)		2.096(9)	Ta(2)···Ta(2)		3.272(2)
Ta(1)–O(2)		2.325(9)	Ta(2)···Ta(2)		4.328(2)
O(3)–Ta(1)–O(2)		108.5(4)	O(1)–Ta(2)–O(1)		171.2(5)
O(3)–Ta(1)–O(5)		100.2(5)	O(1)–Ta(2)–Se(2)		90.3(3)
O(3)–Ta(1)–O(4)		100.2(6)	O(1)–Ta(2)–Se(2)		95.4(3)
O(3)–Ta(1)–O(1)		102.7(4)	O(1)–Ta(2)–Se(1)		86.1(3)
O(3)–Ta(1)–O(2)		174.0(4)	O(1)–Ta(2)–Se(1)		87.0(3)
O(2)–Ta(1)–O(5)		91.6(5)	Se(2)–Ta(2)–Se(2)		100.09(6)
O(2)–Ta(1)–O(4)		94.6(5)	Se(2)–Ta(2)–Se(1)		92.55(5)
O(2)–Ta(1)–O(1)		148.7(4)	Se(2)–Ta(2)–Se(1)		167.26(5)
O(2)–Ta(1)–O(2)		77.5(4)	Se(1)–Ta(2)–Se(1)		74.87(7)
O(5)–Ta(1)–O(4)		155.5(6)	Ta(2)–Se(1)–Ta(2)		105.13(7)
O(5)–Ta(1)–O(1)		80.5(5)	Ta(2)–Se(2)–Ta(2)		79.91(6)
O(5)–Ta(1)–O(2)		79.7(5)	Ta(1)–O(4)–Ta(1)		153.1(9)
O(4)–Ta(1)–O(1)		82.0(5)	Ta(1)–O(5)–Ta(1)		157.1(8)
O(4)–Ta(1)–O(2)		78.5(5)	Ta(1)–O(2)–Ta(1)		102.5(4)
O(1)–Ta(1)–O(2)		71.3(3)	Ta(2)–O(1)–Ta(1)		133.6(5)
O(3)–Pr(1)–O(3)		100.9(5)	O(4)–Pr(2)–O(3)		130.1(2)
O(3)–Pr(1)–O(2)		74.5(3)	O(4)–Pr(2)–O(2)		65.9(3)
O(3)–Pr(1)–O(2)		156.1(3)	O(4)–Pr(2)–O(1)		63.7(3)
O(3)–Pr(1)–O(1)		71.8(3)	O(4)–Pr(2)–Se(1)		106.1(4)
O(3)–Pr(1)–O(1)		140.4(3)	O(4)–Pr(2)–Se(2)		118.3(4)
O(3)–Pr(1)–O(5)		128.5(2)	O(3)–Pr(2)–O(3)		99.9(5)
O(3)–Pr(1)–Se(1)		75.1(2)	O(3)–Pr(2)–O(2)		73.9(3)
O(3)–Pr(1)–Se(2)		71.2(2)	O(3)–Pr(2)–O(2)		147.1(3)
O(2)–Pr(1)–O(2)		100.0(4)	O(3)–Pr(2)–O(1)		71.2(3)
O(2)–Pr(1)–O(1)		61.3(3)	O(3)–Pr(2)–O(1)		149.6(3)
O(2)–Pr(1)–O(1)		126.6(3)	O(3)–Pr(2)–Se(1)		77.8(2)
O(2)–Pr(1)–O(5)		65.4(3)	O(3)–Pr(2)–Se(2)		74.0(2)
O(2)–Pr(1)–Se(1)		81.1(2)	O(2)–Pr(2)–O(2)		93.7(4)
O(2)–Pr(1)–Se(2)		126.7(2)	O(2)–Pr(2)–O(1)		60.1(3)
O(1)–Pr(1)–O(1)		89.2(4)	O(2)–Pr(2)–O(1)		129.2(3)
O(1)–Pr(1)–O(5)		61.3(3)	O(2)–Pr(2)–Se(1)		129.8(2)
O(1)–Pr(1)–Se(1)		135.0(2)	O(2)–Pr(2)–Se(2)		73.1(2)
O(1)–Pr(1)–Se(2)		69.7(2)	O(1)–Pr(2)–O(1)		101.6(4)
O(5)–Pr(1)–Se(1)		125.7(3)	O(1)–Pr(2)–Se(1)		71.9(2)
O(5)–Pr(1)–Se(2)		108.5(3)	O(1)–Pr(2)–Se(2)		127.4(2)
Se(1)–Pr(1)–Se(2)		125.8(1)	Se(1)–Pr(2)–Se(2)		135.7(1)

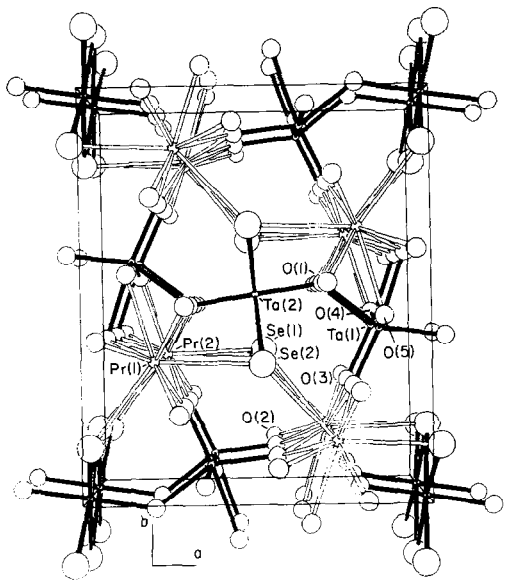

FIG. 2. A labeled view down the c axis of the $Pr_2Ta_3Se_2O_8$ unit cell.

tricapped-trigonal prismatic sites. The greatest axial contraction occurs along the b axis in the series La to Nd. Figure 4 shows one layer of octahedrally coordinated Ta atoms. Atom Ta(2) is in a distorted octahedral site with *trans* O(1) atoms, *cis* Se(1), and *cis* Se(2) atoms. The Ta(1)–O(1) distance is 1.978(9) Å and the Ta(1)–Se distances are 2.548(2) and 2.725(2) Å. These Ta(2) octahedra form a chain of Se edge-shared octahedra in the c direction. There are alternating short–long Ta(2)–Ta(2) separations of 3.272(2) and 4.328(2) Å. This chain of Ta(2) octahedra is corner shared through atom O(1) to the distorted Ta(1) octahedral sites. Atom Ta(1) sits in a distorted octahedral site surrounded by six O atoms with Ta–O distances ranging from 1.834(10) to 2.325(9) Å. These Ta–O distances are comparable to those in $CaTa_2O_6$ (1.85(3)–2.11(2) Å (*20*)). The Ta(1)–O octahedra are edge shared through atoms O(2) in the a direction and corner shared through atoms O(4) and O(5) in the c direction. These chains of Ta–O octahedral dimers are also observed in Ca Ta_2O_6. The edge shared Ta(1)–Ta(1) distance is 3.327(1) Å.

The interatomic distances determined from the neutron data are listed in Table VIII. Even though the neutron data were collected at 298 K and the X-ray data at 111 K the results of the two studies may be compared because of minimal thermal motion in this structure. Indeed, they compare favorably, including distances involving the oxygen atoms. Overall, the X-ray results are of comparable or greater precision.

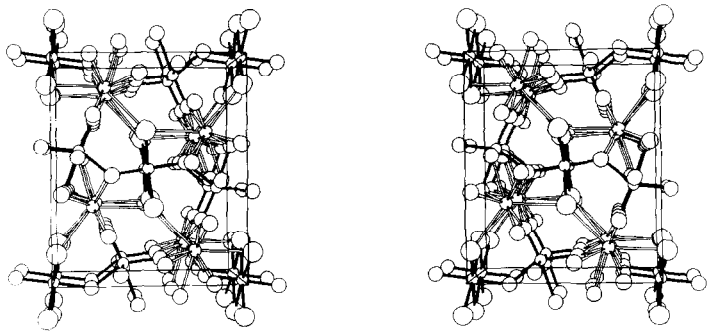

FIG. 3. A stereoview of the structure of $Pr_2Ta_3Se_2O_8$, with the a axis from left to right, the b axis from bottom to top, and the c axis out of the paper. The Ta atoms are small circles with filled bonds; the Pr atoms are small circles with open bonds; the O atoms are medium circles; the Se atoms are large circles.

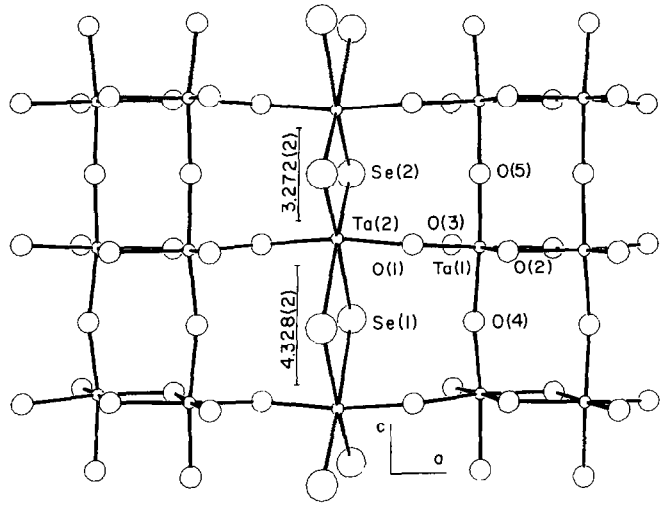

FIG. 4. A view of the Ta-octahedra layers showing the numbering scheme and the alternating long-short Ta(2)–Ta(2) distances.

Physical measurements on $La_2Ta_3Se_2O_8$. Two-probe conductivity measurements indicate that $La_2Ta_3Se_2O_8$ is a poor conductor. Plots of the temperature dependence of the magnetic susceptibility (χ) and of $\chi \cdot T$ vs T at 5 kG are given for $La_2Ta_3Se_2O_8$ in Fig. 5. The magnetic data were corrected for ion-core diamagnetism (*21*) and then fit by a least-squares procedure to the equation

$$\chi = C/(T + \theta) + \chi_0.$$

The values obtained for θ, C, and χ_0 are 0.20(2) K, 0.0117(4) emu · K/mole, and 1.6(1) × 10^4 emu/mole, respectively. The effective magnetic moment from the for-

TABLE VIII

DISTANCES (Å) IN $Pr_2Ta_3Se_2O_8$ FROM NEUTRON DIFFRACTION POWDER DATA

Pr(1)–O(3)	2×	2.539(18)	Pr(2)–O(4)		2.621(23)
Pr(1)–O(2)	2×	2.483(16)	Pr(2)–O(3)	2×	2.447(19)
Pr(1)–O(1)	2×	2.531(15)	Pr(2)–O(2)	2×	2.571(15)
Pr(1)–O(5)		2.456(24)	Pr(2)–O(1)	2×	2.613(13)
Pr(1)–Se(1)		3.098(18)	Pr(2)–Se(1)		2.910(18)
Pr(1)–Se(2)		3.109(18)	Pr(2)–Se(2)		3.000(18)
Pr(1)···Ta(1)		3.394(16)	Pr(2)···Ta(1)		3.494(16)
Ta(1)–O(3)		1.864(7)	Ta(2)–O(1)	2×	1.979(6)
Ta(1)–O(2)		1.949(7)	Ta(2)–Se(2)	2×	2.546(8)
Ta(1)–O(5)		1.934(14)	Ta(2)–Se(1)	2×	2.686(8)
Ta(1)–O(4)		1.933(15)	Ta(1)···Ta(1)		3.284(1)
Ta(1)–O(1)		2.076(7)	Ta(2)···Ta(2)		3.316(2)
Ta(1)–O(2)		2.290(7)	Ta(2)···Ta(2)		4.291(2)

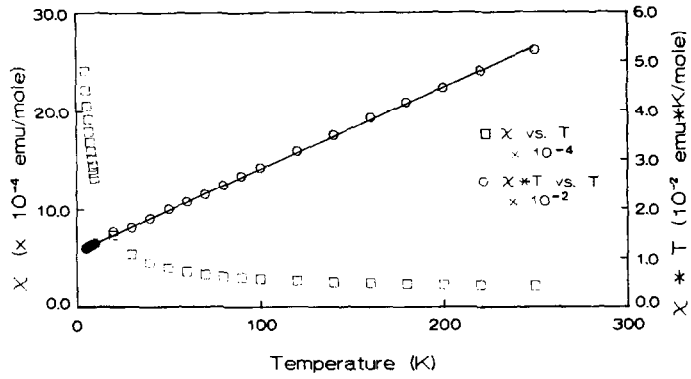

FIG. 5. Plot of χ (□) and $\chi \cdot T$ (○) vs. T.

mula (22) $\mu_{eff} = (8C)^{1/2}$ is 0.30 BM per $La_2Ta_3Se_2O_8$ unit.

Ta oxidation state. In the assignment of formal oxidation states in $Ln_2Ta_3Se_2O_8$ we suggest Ln +3, Se −2, and O −2; this leaves +14 charge units to be divided among three Ta atoms. We believe that atom Ta(1), Wyckoff position 8h, with six-coordinated O atoms may be taken as +5 and that atom Ta(2), Wyckoff position 4e, with two-coordinated O and four-coordinated Se atoms may be taken as +4. Consistent with this view the alternating long–short Ta(2)–Ta(2) distances, 4.328(2) and 3.272(2) Å, may indicate a d^1–d^1 bonding interaction. Such a bonding interaction is likely in view of the small paramagnetic moment and poor conductivity of $La_2Ta_3Se_2O_8$.

The observation of multiple valent Ta and V atoms in $Ln_2Ta_3Se_2O_8$ and $La_5V_3O_7S_6$ and the observation of magnetic exchange in $LnCrOQ_2$ (Q = S, Se) compounds suggest that quarternary transition-metal oxychalcogenides have an exciting potential for new structures with interesting physical properties.

Acknowledgments

This research was supported by the U.S. National Science Foundation—Solid State Chemistry—Grant DMR-88-13623. Use was made of the Scanning Electron Microscope Facility of Northwestern University's Material Research Center, supported by NSF Grant DMR 88-21571. The IPNS facility at Argonne National Laboratory is supported by the U.S. Department of Energy. We thank Drs. Richard Hitterman and Frank Rotella of Argonne National Laboratory for many helpful discussions.

References

1. M. GUITTARD, S. BENAZETH, J. DUGUÉ, S. JAULMES, M. PALAZZI, P. LARUELLE, AND J. FLAHAUT, *J. Solid State Chem.* **51,** 227 (1984).
2. T. OKABE, G. VAN TENDELOO, J. VAN LANDUYT, S. AMELINCKX, AND M. GUITTARD, *J. Solid State Chem.* **72,** 376 (1988).
3. T. VOVAN, M. GUITTARD, J. DUGUÉ, AND J. FLAHAUT, AND A. CHILOUET, *J. Solid State Chem.* **73,** 11 (1988).
4. T. VOVAN, C. ECREPONT, M. GUITTARD, AND J. FLAHAUT, *C.R. Acad. Sci. Ser. II* **304,** 333 (1987).
5. J. DUGUÉ, T. VOVAN, AND J. VILLERS, *Acta Crystallogr. Sect. B* **36,** 1291 (1980).
6. J. DUGUÉ, T. VOVAN, AND J. VILLERS, *Acta Crystallogr. Sect. B* **36,** 1294 (1980).
7. M. WINTENBERGER, T. VOVAN, AND M. GUITTARD, *Solid State Commun.* **53,** 227 (1985).
8. M. WINTENBERGER, J. DUGUÉ, M. GUITTARD, N. H. DUNG, AND T. VOVAN, *J. Solid State Chem.* **70,** 295 (1987).
9. J. DUGUÉ, T. VOVAN, AND P. LARUELLE, *Acta Crystallogr. Sect. C* **41,** 1146 (1985).
10. J. M. WATERS AND J. A. IBERS, *Inorg. Chem.* **16,** 3273 (1977).
11. "International Tables for X-ray Crystallography," Vol. IV, Tables 2.2A and 2.3.1, Kynoch Press, Birmingham (1974).

12. J. A. IBERS AND W. C. HAMILTON, *Acta Crystallogr.* **17,** 781 (1964).
13. G. M. SHELDRICK, in "Crystallographic Computing 3," (G. M. Sheldrick, C. Kruger, and R. Goddard, Eds.), pp. 175–189, Oxford Univ. Press, London (1985).
14. L. M. GELATO AND E. PARTHÉ, *J. Appl. Crystallogr.* **20,** 139 (1987).
15. E. PARTHÉ AND L. M. GELATO, *Acta Crystallogr. Sect. A* **40,** 169 (1984).
16. J. JORGENSEN AND F. ROTELLA, *J. Appl. Crystallogr.* **15,** 27 (1982).
17. R. VON DREELE, J. JORGENSEN, AND C. WINDSOR, *J. Appl. Crystallogr.* **15,** 581 (1982).
18. P. N. IYER AND A. J. SMITH, *Acta Crystallogr.* **23,** 740 (1967).
19. R. J. HILL AND C. J. HOWARD, *J. Appl. Crystallogr.* **20,** 467 (1987).
20. L. JAHNBERG, *Acta Chem. Scand.* **71,** 2548 (1963).
21. L. N. MULAY AND E. A. BOUDREAUX, (Eds.), "Theory and Application of Molecular Diamagnetism," Wiley–Interscience, New York (1970).
22. J. M. VAN DEN BERG AND P. COSSEE, *Inorg. Chim. Acta* **2,** 143 (1968).
23. J. DE MEULENAER AND H. TOMPA, *Acta Crystallogr.* **19,** 1014 (1965).
24. J. C. HUFFMAN, Ph.D. thesis, Indiana University (1974).
25. P. G. LENHERT, *J. Appl. Crystallogr.* **8,** 568 (1975).